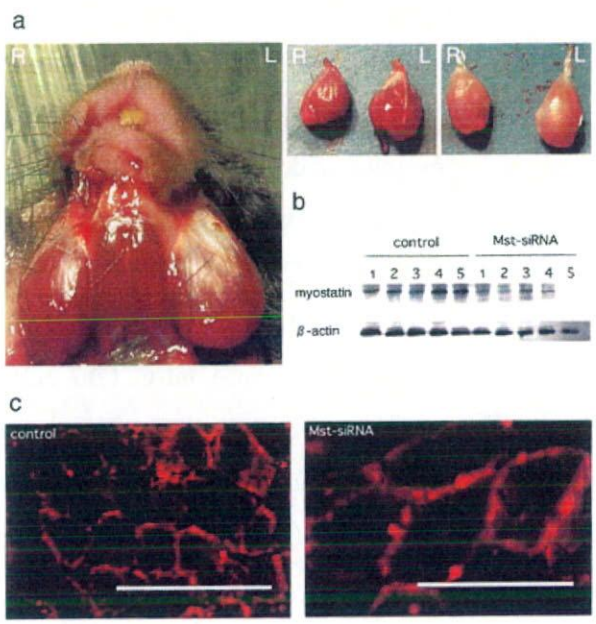
a
R
L
R
L
R
L
b
control
Mst-siRNA
1 2 3 4 5 1 2 3 4 5
myostatin
β-actin
c
control
Mst-siRNA

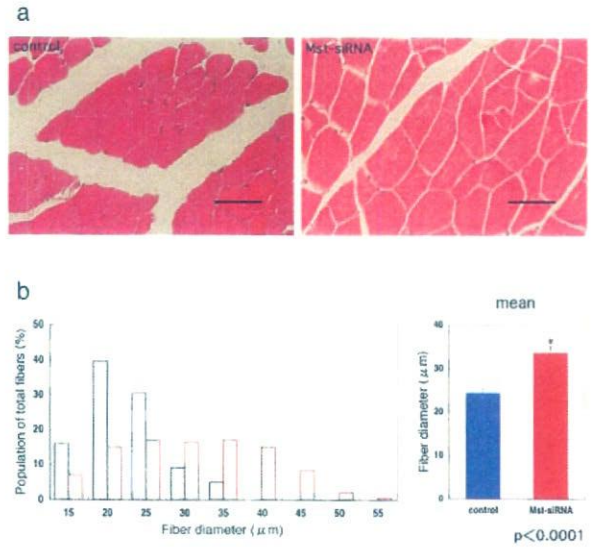
a
control
Mst-siRNA
b
mean
Population of total fibers (%)
Fiber diameter (μm)
Fiber diameter (μm)
control
Mst-siRNA
p<0.0001

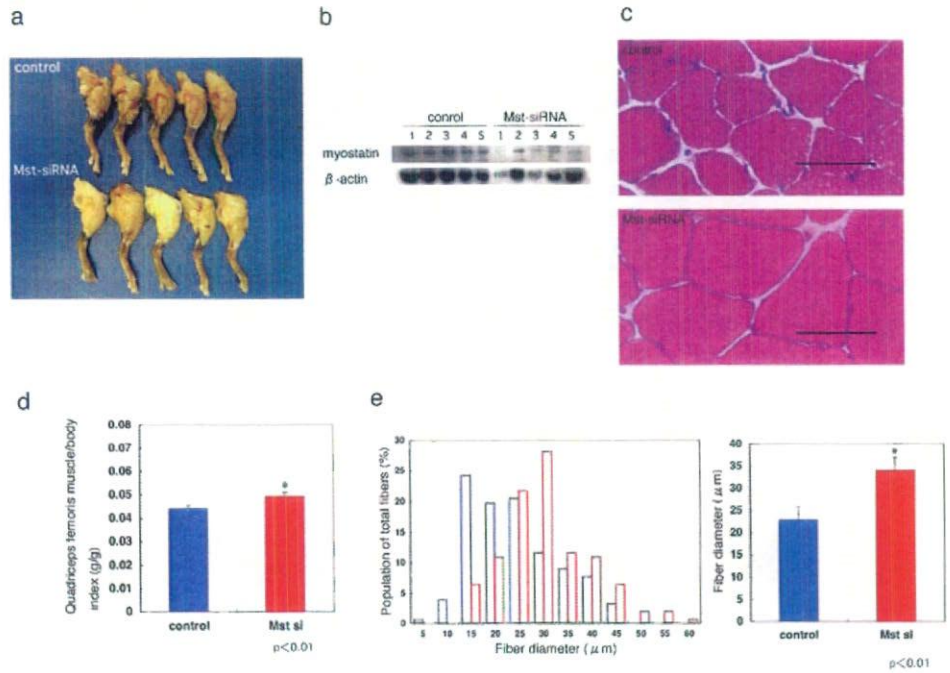
a
control
Mst-siRNA
b
conrol
Mst-siRNA
1 2 3 4 5 1 2 3 4 5
myostatin
β -actin
c
control
Mst-siRNA
d
Quadriceps femoris muscle/body index (g/g)
0.08
0.07
0.06
0.05
0.04
0.03
0.02
0.01
0
control
Mst si
p<0.01
e
Population of total fibers (%)
Fiber diameter ( μ m)
Fiber diameter ( μ m)
control
Mst si
p<0.01

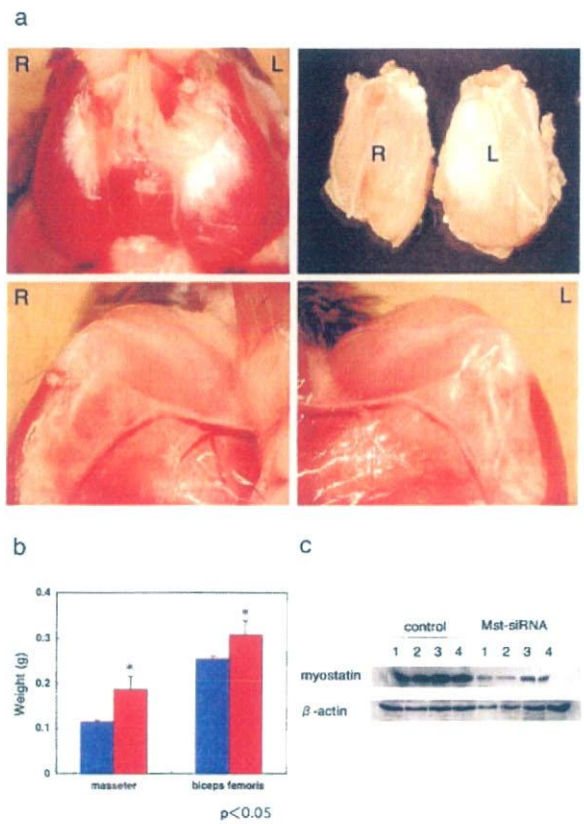
a
R
L
R
L
R
L
b
c
Weight (g)
0.4
0.3
0.2
0.1
0
masseter
biceps femoris
p<0.05
control
Mst-siRNA
1 2 3 4 1 2 3 4
myostatin
β-actin

ARTHRITIS & RHEUMATISM
Vol. 58, No. 2, February 2008, pp 389–400
DOI 10.1002/art.23163


# Effective Treatment With Oral Administration of Rebamipide in a Mouse Model of Sjögren's Syndrome

Masayuki Kohashi,[1] Naozumi Ishimaru,[2] Rieko Arakaki,[2] and Yoshio Hayashi[2]

*Objective.* **To determine whether oral administration of rebamipide, a mucosal protective agent, is effective in the treatment of Sjögren's syndrome (SS) in the NFS/*sld* mouse model of the disease.**

*Methods.* **NFS/*sld* mice were given daily oral doses of rebamipide (0.3 mg/kg of body weight or 3 mg/kg) or vehicle alone starting from the age of 4 weeks to the age of 8 weeks. The volume of saliva and tears was monitored during and after treatment. After the final dose, histologic features of the tissues, TUNEL+ apoptotic duct cells in affected glands, T cell and cytokine function, and levels of immunoglobulin isotypes and serum autoantibodies were examined.**

*Results.* **The 3-mg/kg dose of rebamipide prevented the development of autoimmune lesions. The average volume of saliva in rebamipide-treated mice was significantly higher than that in control mice. We found decreased TUNEL+ apoptotic duct cells in the salivary and lacrimal glands of rebamipide-treated mice as compared with control mice. Rebamipide treatment suppressed the activation of CD4+ T cells and Th1 cytokines (interleukin-2, interferon-γ) associated with impaired NF-κB activity. Production of serum autoantibodies, IgM, and IgG1 was clearly inhibited.**

*Conclusion.* **Our findings demonstrate the efficacy of oral administration of rebamipide in the treatment of SS. Rebamipide represents a new therapeutic strategy for the treatment of patients with sicca symptoms caused by SS, as well as for patients with other diseases.**

Sjögren's syndrome (SS) is an autoimmune disorder characterized by lymphocytic infiltrates and destruction of the salivary and lacrimal glands, as well as systemic production of autoantibodies to the RNP particles SSA/Ro and SSB/La (1–3). Although the specificity of cytotoxic T lymphocyte function has been an important issue in studies of organ-specific autoimmune responses, the mechanisms responsible for tissue destruction in SS remain to be fully elucidated. The immune system has acquired regulatory mechanisms that preclude the reactivity of mature T cells to self antigens presented by major histocompatibility complex (MHC) molecules, while maintaining an ability to respond to non-self antigens presented by self MHC molecules (4,5). The dysregulation of T cell tolerance is considered to be responsible for many types of autoimmune diseases, and a variety of mechanisms involved in the initiation of autoimmune diseases have been proposed (6–10).

Data from our previous studies demonstrated that autoreactive CD4+ T cells play a pivotal role in the development of autoimmune exocrinopathy in the NFS/*sld* mouse model of SS (11). It is now evident that the interaction of Fas with FasL regulates a large number of pathophysiologic processes of apoptosis, including autoimmune diseases (11,12). Previous studies have also confirmed the observation that apoptotic cells in various cell types are implicated as the source of autoantigen when stimulated with different proapoptotic stimuli (13).

On the other hand, natural autoantibody appears to be primarily IgM polyreactive antibody of low affinity, which is quite different from the monospecific high-affinity IgG antibody usually associated with autoimmune disease (14). It is important to note that au-

Supported in part by the Ministry of Education, Science, Sports, and Culture of Japan (Grants-in-Aid for Scientific Research 17109016 and 17689049) and the Uehara Memorial Foundation.

[1]Masayuki Kohashi, PhD: University of Tokushima Graduate School, and Otsuka Pharmaceutical Company, Ltd., Tokushima, Japan; [2]Naozumi Ishimaru, DDS, PhD, Rieko Arakaki, PhD, Yoshio Hayashi, DDS, PhD: University of Tokushima Graduate School, Tokushima, Japan.

Address correspondence and reprint requests to Yoshio Hayashi, DDS, PhD, Department of Oral Molecular Pathology, Institute of Health Biosciences, University of Tokushima Graduate School, 3 Kuramoto-cho, Tokushima 770-8504, Japan. E-mail: hayashi@dent.tokushima-u.ac.jp.

Submitted for publication June 15, 2007; accepted in revised form October 26, 2007.

toantigens released from the intracytoplasmic environment will not, under normal conditions, stimulate the production of pathogenic IgG autoantibodies capable of causing tissue damage (14,15). During an autoimmune disease, levels of IgM autoantibodies are high (16) due to the stimulation of IgM autoantibody–producing cell lines by the release of autoantigens from target cells. IgG antibodies are the primary mediators of protective humoral immunity against pathogens, but they can also be pathogenic. Acting as cytotoxic molecules or as immune complexes, IgG autoantibodies are the principal mediators of autoimmune diseases such as idiopathic thrombocytopenia, autoimmune hemolytic anemia, and systemic lupus erythematosus, and may contribute to other autoimmune diseases, such as rheumatoid arthritis, type 1 diabetes mellitus, and multiple sclerosis (17).

Rebamipide (2-[4-chlorobenzoylamino]-3-[2(1*H*)quinolinon-4-yl]propionic acid; OPC-12759) is a mucosal protective agent used for the treatment of gastritis and gastric ulcer. It has recently been reported that rebamipide works as an antiinflammatory agent in both acute and chronic inflammation and has an inhibitory effect on proinflammatory cytokines (18). Experimental data have shown that rebamipide can prevent Dextran sulfate sodium–induced colitis in rats (19). A recent study demonstrated the protective effect of rebamipide on the intestinal barrier, namely, its ability to reinforce the epithelial barrier capacity and to decrease macromolecular transport across this barrier (20). At the same time, the study demonstrated the immunoregulatory properties of rebamipide, which is capable of regulating lymphocyte proliferation and cytokine secretion (20).

The aim of the present study was to investigate the effects of oral administration of rebamipide on various parameters of autoimmune responses and on serum levels of autoantibodies, immunoglobulins, and inflammatory cytokines in a murine model of SS. We hypothesized that in this model of SS, the immunomodulatory activity of rebamipide against autoimmune responses to tissue-specific autoantigens would be a good therapeutic approach.

## MATERIALS AND METHODS

**Mice and experimental design.** Female mice of the NFS/N strain carrying the mutant gene *sld* (21) were reared in our specific pathogen–free mouse colony and given food and water ad libitum. Thymectomy was performed on day 3 after birth in the NFS/*sld* mice (22). A total of 35 NFS/*sld* mice that had been subjected to thymectomy on day 3 after birth were investigated in the present study. An additional group of 10 mice not subjected to thymectomy were also investigated. Rebamipide (Otsuka Pharmaceutical, Tokushima, Japan) was prepared as a suspension in 0.5% carboxymethylcellulose (Dai-Ichi Chemical Industries, Tokyo, Japan) in water.

The following experimental groups were studied: a vehicle-treated control group, which received oral administration of vehicle alone (n = 12), and 2 rebamipide-treated groups, which received oral administration of rebamipide at a dose of either 0.3 mg/kg of body weight (n = 12) or 3 mg/kg of body weight (n = 11). Thymectomized NFS/*sld* mice were given daily oral treatment with rebamipide or vehicle, starting from the age of 4 weeks to age 8 weeks. Nonthymectomized mice (n = 10) received oral administration of vehicle alone.

OT-2 mice (C57BL/6-Tg[TcraTcrb]452Cbn/J) were obtained from Dr. J. Sprent (Garvan Institute of Medical Research, Darlinghurst, New South Wales, Australia). These mice (n = 5) were used in the transfer experiment.

All experiments were approved by the Animal Ethics Board of the University of Tokushima.

**Histologic assessment.** At the end of the treatment period, all organs were removed from the mice, fixed in 4% phosphate buffered formaldehyde (pH 7.2), and prepared for histologic examination. Formalin-fixed tissue sections were stained with hematoxylin and eosin, and 3 pathologists (NI, RA, and YH) independently evaluated the histologic features without knowledge of the condition of each mouse. Histologic changes were scored on a scale of 1–3, where 1 = no change or slight lymphoid cell infiltration (slight), 2 = mild lymphoid cell infiltration (moderate), and 3 = marked lymphoid cell infiltration with tissue destruction (severe). Histologic evaluation was performed in a blinded manner, and 1 tissue section from each salivary and lacrimal gland was evaluated.

**TUNEL assay.** Apoptotic cells were detected in tissue sections using the in situ TUNEL kit (Wako Pure Chemical, Osaka, Japan), as previously described (23). Briefly, sections were incubated with proteinase K (400 mg/ml) for 5 minutes, and then presoaked for 10 minutes in terminal deoxynucleotidyl transferase (TdT) buffer (0.5 $\mu$moles/liter of cacodylate, 1 mmole/liter of $CoCl_2$, 0.5 $\mu$moles/liter of dithiothreitol, 0.05% bovine serum albumin, 0.15 moles/liter of NaCl). Sections were incubated for 2 hours at 37°C in 25 $\mu$l of TdT solution containing 1× terminal transferase buffer, 0.5 nmoles of biotin-labeled dUTP, and 10 units of TdT.

After the TdT reaction, sections were soaked in TdT blocking buffer (300 nmoles/liter of NaCl, 30 mmoles/liter of trisodium citrate-2-hydrate), incubated with horseradish peroxidase (HRP)–conjugated streptavidin for 30 minutes at room temperature, and developed for 10 minutes in phosphate buffered citrate (pH 5.8) containing 0.6 mg/ml of 3,3′-diaminobenzidine tetrahydrochloride dihydrate (DAB). Nuclei were counterstained with methyl green.

**Flow cytometric analysis.** Surface markers were identified with monoclonal antibodies (mAb) and using an Epics flow cytometer (Beckman Coulter, Miami, FL). Rat mAb against fluorescein isothiocyanate (FITC)–, phycoerythrin (PE)–, or PE-Cy5–conjugated anti-B220, Thy1.2, CD4, and CD8 (eBioscience, San Diego, CA) were used. For detection of T cell activation makers, FITC-conjugated anti-CD25, anti-CD44, anti-CD62L, and anti-CD69 mAb (eBioscience) were used. For detection of B cell surface IgM and IgG1, FITC-conjugated anti-IgM (eBioscience) and anti-IgG1 (BD Phar-

Mingen, San Diego, CA) mAb were used. PE-conjugated anti-Ly5.2 (eBioscience) and biotin-conjugated anti-$V_\beta$5.2 and PE-Cy5–conjugated streptavidin (both from BD PharMingen) were used for in vivo ovalbumin-specific T cell expansion. Data were analyzed with FlowJo FACS analysis software (Tree Star, Ashland, OR).

**Transfer of OT-2 T cells.** Purified CD4+ T cells ($5 \times 10^6$) derived from the spleen of transgenic OT-2 mice were labeled with carboxyfluorescein succinimidyl ester (CFSE; Molecular Probes, Eugene, OR) and transferred intravenously into B6 (Ly5.1+) mice. One day later, ovalbumin peptide (100 $\mu$g) was injected intraperitoneally and rebamipide (0–200 $\mu M$; 250 $\mu$l per mouse) was injected intravenously into recipient mice. Three days later, cell division was evaluated by flow cytometry to detect the CFSE dilution of the Ly5.2+,$V_\beta$5.2+, CD4+ T cells.

**Real-time quantitative reverse transcription–polymerase chain reaction analysis.** Total RNA was extracted from cultured T cells and B cells derived from the spleen of NFS/*sld* mice with Isogen (Wako Pure Chemical), and reverse transcribed. Transcript levels of NF-κB, FasL, interferon regulatory factor 4 (IRF-4), B lymphocyte–induced maturation protein 1 (BLIMP-1), and β-actin were determined with a PTC-200 DNA Engine Cycler (MJ Research, Waltham, MA) with SYBR Premix Ex Tag (Takara, Kyoto, Japan). The following primer sequences were used: for NF-κB, 5′-ATGGCAGACGATGATCCCTA-3′ (forward) and 5′-TAGGCAAGGTCAGAATGCAC-3′ (reverse); for FasL, 5′-ACTGGACAGATATGGGCCCAC-3′ (forward) and 5′-GCCTCTGTGAGGTAGTAAGTAG-3′ (reverse); for IRF-4, 5′-GAAGCCCCAAAGCCCTCAGTCGTTG-3′ (forward) and 5′-CGCTGAGGAGGAAACTGAA-3′ (reverse); for BLIMP-1, 5′-CATTCCTGTCCCCAACGCATCAACTG-3′ (forward) and 5′-GGTGCCCAAGCACCAAAGTCATAG-3′ (reverse); and for β-actin, 5′-GTGGGCCGCTCTAGGCACCA-3′ (forward) and 5′-CGGTTGGCCTTAGGGTTCAGGGGGG-3′ (reverse). Results were calculated with DNA Engine Opicon System software (Roche Molecular Systems, Alameda, CA).

**Western blot analysis.** Cell extracts from the nucleus and cytoplasm of T cells and B cells were prepared using a Nuclear/Cytosol Fractionation kit (BioVision, Mountain View, CA). Cells were briefly washed, collected in ice-cold phosphate buffered saline (PBS) in the presence of phosphatase inhibitors, and centrifuged at 500 revolutions per minute for 5 minutes. The pellets were resuspended in a hypotonic buffer, treated with detergent, and centrifuged at 14,000*g* for 30 seconds. The cytoplasmic fraction was collected, the nuclei were lysed, and nuclear proteins were solubilized in lysis buffer containing protease inhibitors. A total of 10 $\mu$g of each sample per well was used for sodium dodecyl sulfate–polyacrylamide gel electrophoresis. After blocking with 5% nonfat milk, the membrane was incubated with primary antibodies against phospho-IκBα and NF-κB p65 (RelA) (Santa Cruz Biotechnology, Santa Cruz, CA). Antigen–antibody complexes were detected using a HRP-conjugated secondary antibody. Protein binding was visualized with enhanced chemiluminescence Western blotting reagent (Amersham Biosciences, Arlington Heights, IL). Anti-mouse histone H1 or GAPDH monoclonal antibody (Santa Cruz Biotechnology) was used as the control for protein loading.

**Measurement of fluid secretion.** Analysis of tear and saliva volumes in rebamipide-treated thymectomized NFS/*sld* mice was performed according to a previously described method (24).

**Proliferation assay.** CD4+ T cells ($1 \times 10^5$) purified from spleen cells using anti-B220 mAb, anti-CD8 mAb, and anti-rat IgG conjugated to magnetic beads (Dynal, Oslo, Norway) were placed in RPMI 1640 containing 10% fetal calf serum (FCS), 100 units/ml of penicillin, 0.1 mg/ml of streptomycin, and 50 $\mu M$ 2-mercaptoethanol and were stimulated with recombinant α-fodrin protein (JS-1) (25) or with plate-coated anti-CD3 and anti-CD28 mAb in 96-well, flat-bottomed plates for 72 hours. Then, $^3$H-thymidine (1 $\mu$Ci/well; NEN Life Science Products, Boston, MA) was pulsed into the cell mixture during the final 20 hours of culture. Incorporation of $^3$H-thymidine was assayed with an automated liquid scintillation counter.

For detection of the proliferation of the CD4+ T cell subset, CFSE-labeled CD4+ T cells were cultured for 72 hours. The CD4+ T cells were then stained with anti-CD4 mAb, and cell division of the CD4+ gated T cells was analyzed by flow cytometer.

**Assay of immunoglobulin secretion from B cells.** B cells ($1 \times 10^5$) purified from spleen cells using anti-CD4 mAb, anti-CD8 mAb, and anti-rat IgG conjugated to magnetic beads (Dynal) were placed in RPMI 1640 containing 10% FCS, penicillin/streptomycin, and 2-mercaptoethanol and were stimulated with 10 $\mu$g/ml of lipopolysaccharide (LPS; Sigma, St. Louis, MO) and 50 ng/ml of interleukin-4 (IL-4; eBioscience) in 96-well round-bottomed plates for 5 days. Cell surface expression of IgM and IgG1 was detected by flow cytometric analysis, and secreted IgM and IgG1 in the culture supernatants were measured by enzyme-linked immunosorbent assay (ELISA).

**Serum autoantibody and cytokine ELISAs.** JS-1, SSA/Ro, SSB/La, or single-stranded DNA (ssDNA) antibody was used to coat 96-well plates (24). After the plates were washed, diluted mouse sera were added. HRP-conjugated anti-mouse IgG (heavy and light chains; Vector, Burlingame, CA) was added as the secondary antibody, and *o*-phenylenediamine (OPD; Sigma) buffer was added. Antibodies were measured with an ELISA reader (Model 680; Bio-Rad, Richmond, CA) and with a spectrophotometer at 490 nm.

Serum immunoglobulins were determined by ELISA using a mouse immunoglobulin quantitation kit (Bethyl Laboratories, Montgomery, TX). Briefly, for the IgM and IgA ELISAs, sera were diluted 1:5,000 in PBS, and for the IgG ELISA, sera were diluted 1:25,000 in PBS. Plates were coated with a capture antibody and then washed with PBS–0.1% Tween 20. Diluted sera or culture supernatants were added to the plates and incubated. After washing with PBS–0.1% Tween 20, an HRP-conjugated detection antibody was added. Plates were again washed with PBS–0.1% Tween 20, and OPD buffer was added. Plates were then analyzed with a spectrophotometer at 490 nm, as described previously (26).

Levels of IL-2, interferon-γ (IFNγ), IL-4, and IL-10 in culture supernatants from splenic CD4+ T cells stimulated with anti-CD3 and anti-CD28 for 72 hours were determined by ELISA. Specific antibodies for each cytokine were used in the ELISAs, as previously described (27).

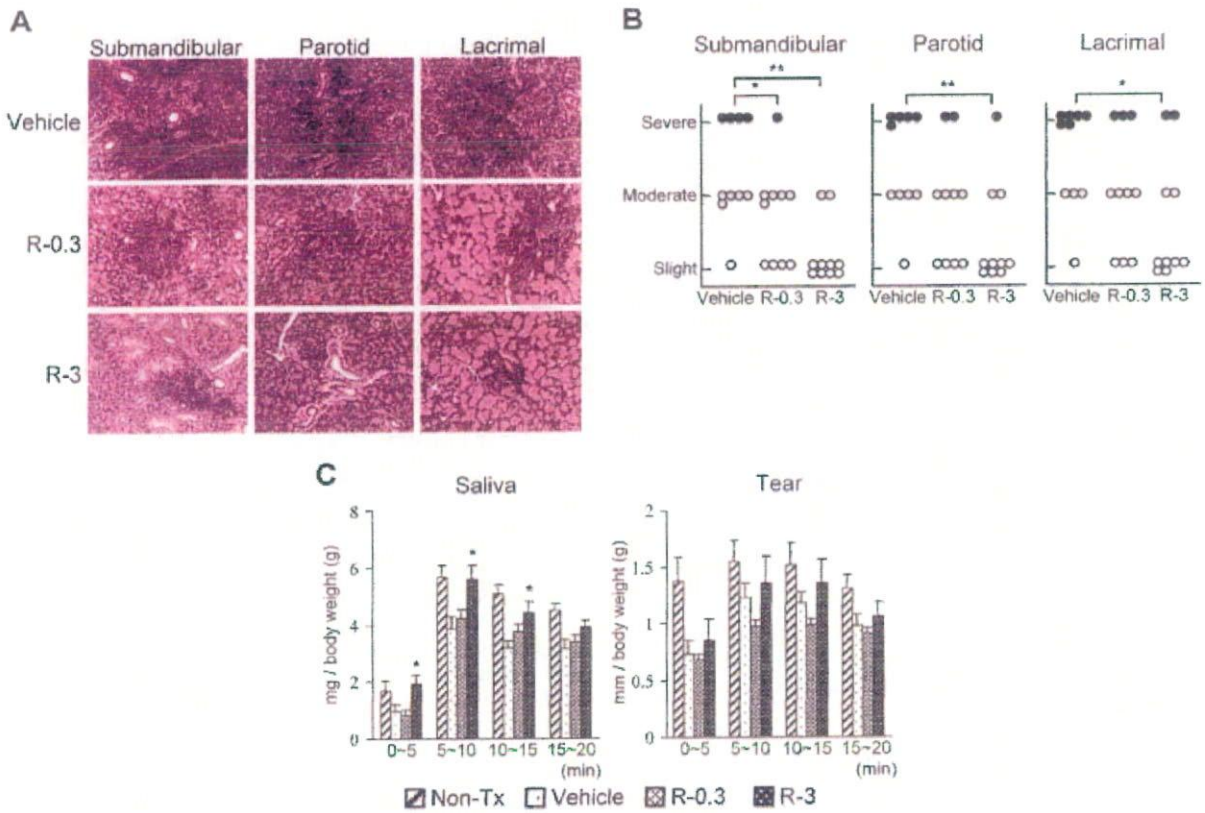


**Figure 1.** Therapeutic effect of rebamipide on autoimmune lesions in the NFS/*sld* mouse model of Sjögren's syndrome. Mice underwent thymectomy on day 3 after birth and were treated with vehicle, 0.3 mg/kg of rebamipide (R-0.3), or 3 mg/kg of rebamipide (R-3) from age 4 weeks to age 8 weeks. **A,** Sections of salivary and lacrimal glands from the 3 groups of mice. Results are representative of 10 mice per group (hematoxylin and eosin stained; magnification × 100). **B,** Histologic grading of inflammatory lesions in salivary and lacrimal glands from individual mice in the 3 treatment groups. * = $P < 0.05$; ** = $P < 0.01$ by lower-tailed Shirley-Williams test. The mean ± SD histology sores in the vehicle, rebamipide 0.3 mg/kg, and rebamipide 3 mg/kg groups were 2.3 ± 0.7, 1.7 ± 0.7, and 1.2 ± 0.4 for the submandibular glands, 2.4 ± 0.7, 1.8 ± 0.8, and 1.4 ± 0.7 for the parotid glands, and 2.5 ± 0.7, 2.0 ± 0.8, and 1.6 ± 0.8 for the lacrimal glands, respectively. **C,** Average saliva and tear volumes after pilocarpine administration (5 mg/kg) in mice of the 3 treatment groups and in a group of nonthymectomized (non-Tx), vehicle-treated mice at different time periods after pilocarpine administration. Values are the mean and SEM of 10–12 mice per group. * = $P < 0.05$ versus the vehicle-treated control group, by Dunnett's test.

**Statistical analysis.** Statistical analysis was performed using the Jonckheere trend test and the lower-tailed Shirley-Williams test, Dunnett's test, Student's *t*-test, and chi-square test, as appropriate.

## RESULTS

**Therapeutic effect of oral administration of rebamipide.** In our previous study (22), we found that NFS/*sld* mice subjected to thymectomy on day 3 after birth began to develop autoimmune lesions of the salivary and lacrimal glands at 4 weeks of age or later, while no inflammatory lesions were observed in nonthymectomized NFS/*sld* mice. In the present study, we investigated whether oral administration of rebamipide protects NFS/*sld* mice against the development of autoimmune lesions. To evaluate whether rebamipide treatment was effective at preventing the SS autoimmune pathology, the drug or vehicle alone was administered orally each day to thymectomized NFS/*sld* mice beginning at the age of 4 weeks and continuing to the age of 8 weeks, then organs were removed for histologic analysis.

Salivary and lacrimal glands were stained with hematoxylin and eosin, and histologic features were assessed. Treatment with rebamipide at a concentration of 3 mg/kg prevented the development of autoimmune

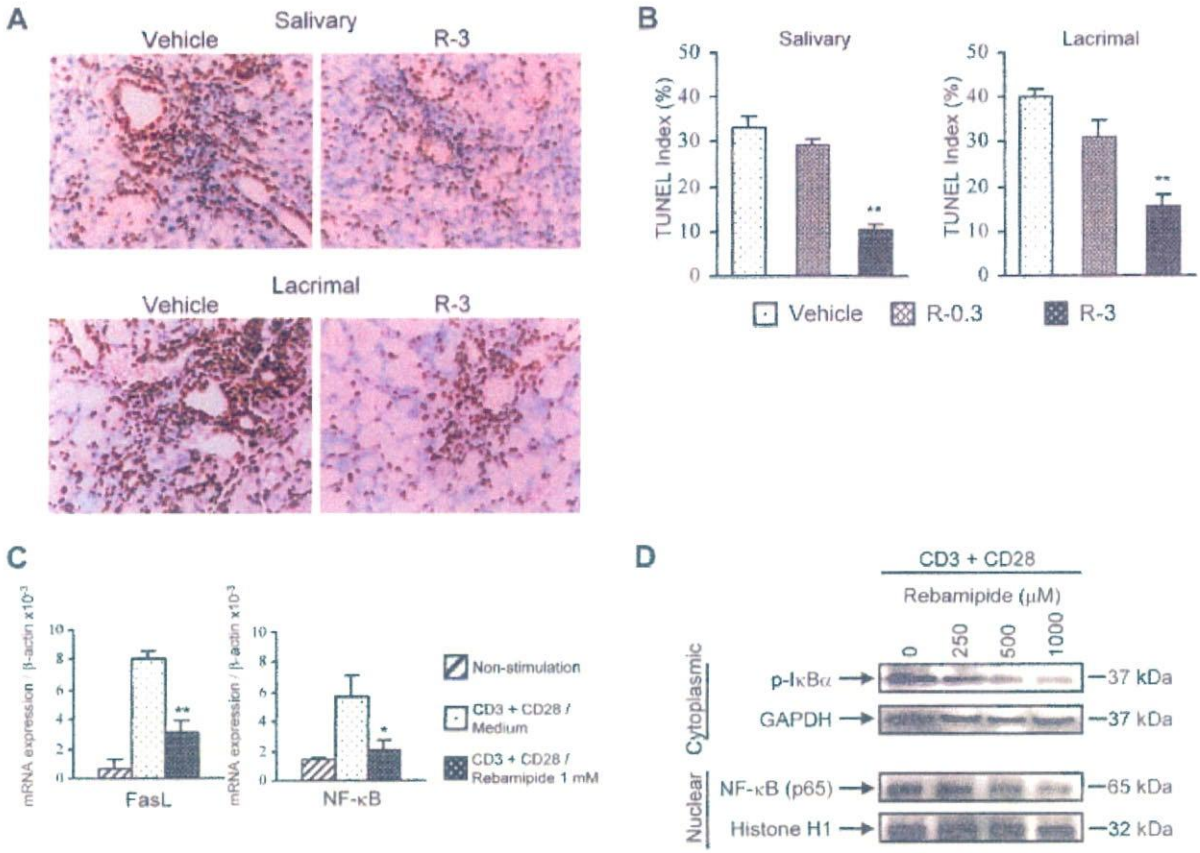


**Figure 2.** Inhibitory effect of rebamipide on apoptosis of salivary gland cells in the NFS/*sld* mouse model of Sjögren's syndrome. Mice underwent thymectomy on day 3 after birth and were treated with vehicle, 0.3 mg/kg of rebamipide (R-0.3), or 3 mg/kg of rebamipide (R-3) from age 4 weeks to age 8 weeks. **A,** TUNEL assay for apoptotic cells in the salivary and lacrimal glands of mice treated with vehicle or with 3 mg/kg of rebamipide. Results are representative of 5–8 mice per group (magnification × 100). **B,** Percentages of TUNEL+ salivary and lacrimal epithelial cells in the 3 treatment groups. Positive cells were enumerated using a 10 × 20–μm grid net disc covering an objective area of 0.16 $mm^2$ (n = 10 fields per section). Values are the mean and SEM of 5 mice per group. ** = $P < 0.01$ versus the vehicle-treated group, by Dunnett's test. **C,** Inhibitory effect of rebamipide on T cell activation. Purified CD4+ T cells derived from mouse spleens were stimulated with plate-coated anti-CD3 and anti-CD28 monoclonal antibody for 2 hours in the presence of rebamipide. Levels of mRNA for FasL and NF-κB were detected by quantitative reverse transcription–polymerase chain reaction analysis. Values are the mean and SEM expression relative to β-actin mRNA in triplicate wells. * = $P < 0.01$; ** = $P < 0.05$ versus medium containing anti-CD3 and anti-CD28, by Student's *t*-test. **D,** Phosphorylation of IκB and nuclear translocation of NF-κB in cytoplasmic and nuclear extracts of activated CD4+ T cells treated with CD3 and CD28 ligation in the presence of rebamipide, as analyzed by Western blotting. GAPDH and histone H1 were used as the respective internal controls. Results are representative of 3 independent experiments.

lesions in the submandibular ($P < 0.01$), parotid ($P < 0.01$), and lacrimal ($P < 0.05$) glands (Figures 1A and B). Rebamipide treatment at a concentration of 0.3 mg/kg prevented the development of autoimmune lesions in the submandibular glands alone ($P < 0.05$). Mononuclear cell infiltration as well as destruction of the parenchyma was inhibited in the salivary and lacrimal glands of thymectomized NFS/*sld* mice treated with rebamipide. The average saliva volume, but not tear volume, in the rebamipide-treated group was significantly higher than that in the vehicle-treated control group (Figure 1C).

We previously demonstrated that epithelial cell apoptosis via the Fas/FasL system plays an important role in the development of autoimmune lesions in this mouse model of SS, and a significant increase in TUNEL+ apoptotic epithelial duct cells in the salivary glands was detected in this mouse model (11). In the

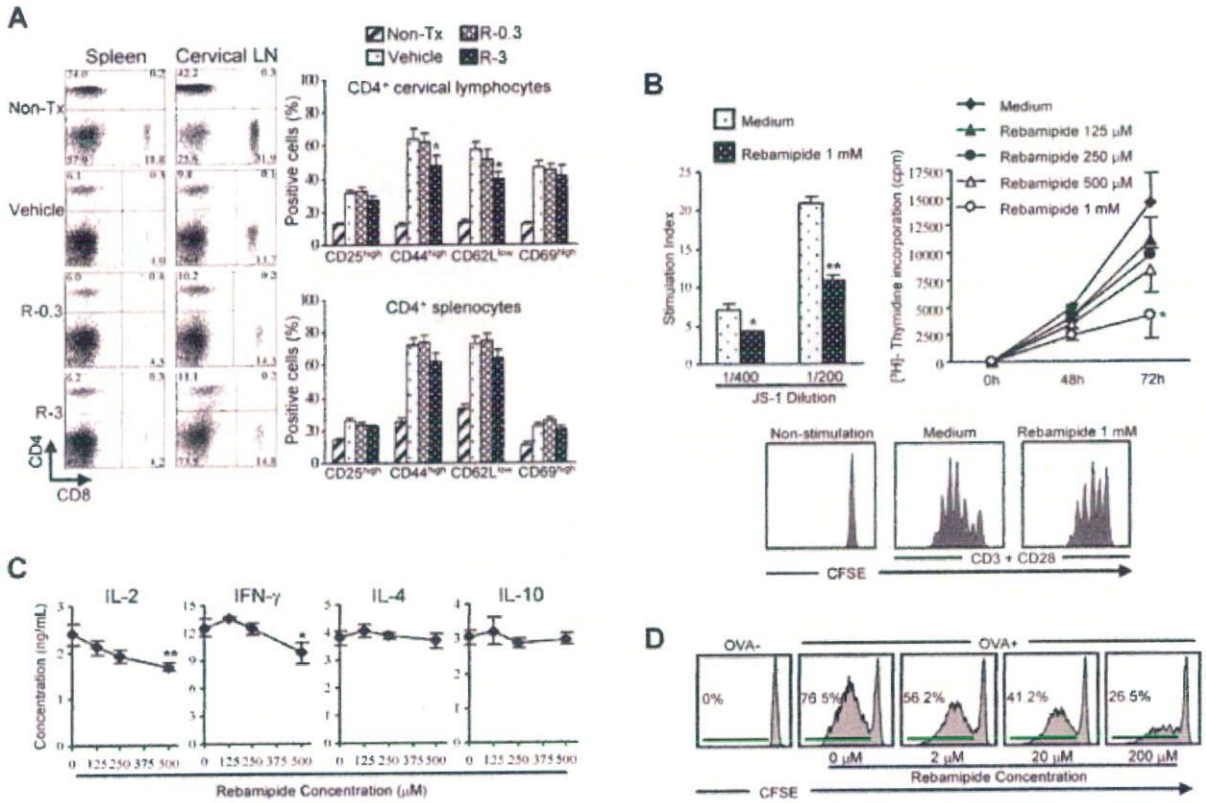


**Figure 3.** Effect of rebamipide on T cell phenotypes and functions in the NFS/*sld* mouse model of Sjögren's syndrome. Mice underwent thymectomy on day 3 after birth and were treated with vehicle, 0.3 mg/kg of rebamipide (R-0.3), or 3 mg/kg of rebamipide (R-3) from age 4 weeks to age 8 weeks. A group of nonthymectomized (non-Tx), vehicle-treated mice was also studied. **A,** CD4+ and CD8+ T cell subsets in the spleen and cervical lymph nodes of the 4 groups of mice, as analyzed by flow cytometry (left). Numbers shown in each compartment are the percentage of positive cells. Results are representative of 10 mice per group. Memory markers on CD4+ T cells derived from the cervical lymph nodes and spleen of the 4 groups of mice were also analyzed by flow cytometry (right). Values are the mean and SEM of 10 mice per group. **B,** Antigen-specific and nonspecific T cell responses. Purified CD4+ T cells from the spleen of thymectomized mice were cultured for 72 hours with irradiated T cell–depleted splenocytes in the presence of recombinant α-fodrin (JS-1), with and without rebamipide (top left). Values are the mean and SEM. * = $P < 0.05$; ** = $P < 0.01$ versus medium alone, by Dunnett's test. Incorporation of $^3$H-thymidine into purified CD4+ T cells stimulated with anti-CD3 and anti-CD28 monoclonal antibodies (mAb) and treated for 48 or 72 hours with the indicated concentrations of rebamipide or medium alone was determined during the last 12 hours of culture (top right). Results are representative of 3 independent experiments. Values are the mean and SEM of triplicate wells. In addition, CD4+ T cells were labeled with carboxyfluorescein succinimidyl ester (CFSE) and were left unstimulated or were stimulated with anti-CD3 and anti-CD28 mAb for 72 hours in the presence of medium alone or 1 m*M* rebamipide (bottom). Cell division was analyzed by flow cytometry. * = $P < 0.01$ versus medium alone, by Dunnett's test. **C,** Production of interleukin-2 (IL-2), interferon-γ (IFNγ), IL-4, and IL-10 by CD4+ T cells stimulated for 72 hours with anti-CD3 and anti-CD28 mAb in the presence of medium alone or the indicated concentrations of rebamipide, as determined by enzyme-linked immunosorbent assay of culture supernatants. Results are representative of 3 independent experiments. Values are the mean ± SEM of triplicate samples. * = $P < 0.05$; ** = $P < 0.01$ versus medium alone, by Dunnett's test. **D,** Flow cytometry of CFSE-labeled CD4+ T cells ($5 \times 10^6$) derived from transgenic OT-2 mice and transferred intravenously into B6 (Ly5.1+) mice. Ovalbumin (OVA) peptide (100 μg) was injected intraperitoneally, and rebamipide (0–200 μ*M*) was injected intravenously, into recipient mice. After 3 days, the CFSE dilution of Ly5.2+,$V_\beta$5.2+,CD4+ T cells was analyzed. Results are representative of 3–5 mice per group.

present study, we observed a decrease in TUNEL+ apoptotic epithelial cells in the salivary glands of mice treated with rebamipide as compared with those in vehicle-treated mice (Figures 2A and B). Indeed, expression of FasL and NF-κB genes on CD4+ T cells was significantly inhibited by rebamipide treatment (Figure 2C), possibly being consistent with the finding of decreased TUNEL+ epithelial cell apoptosis in the

**Table 1.** Autoantibody production in the NFS/*sld* mouse model of Sjögren's syndrome after treatment with rebamipide or vehicle alone*

| Antibody | No. (%) of nonthymectomized, vehicle-treated mice (n = 10) | Treatment in thymectomized mice | | |
|---|---|---|---|---|
| | | No. (%) receiving vehicle (n = 12) | No. (%) receiving 0.3 mg/kg of rebamipide (n = 12) | No. (%) receiving 3 mg/kg of rebamipide (n = 11) |
| SSA/Ro | 0 (0) | 12 (100) | 11 (92) | 8 (73)† |
| SSB/La | 0 (0) | 11 (92) | 10 (83) | 6 (55)† |
| JS-1 | 0 (0) | 7 (58) | 4 (33) | 4 (36) |
| ssDNA | 0 (0) | 11 (92) | 12 (100) | 7 (64) |

* Mice were subjected to thymectomy on day 3 after birth. Autoantibodies were detected by enzyme-linked immunosorbent assay of sera obtained at the end of treatment (8 weeks of age). A positive result was defined as a value higher than the mean ± 3SD of the optical density value in nonthymectomized NFS/*sld* mice. JS-1 is an α-fodrin–specific antibody. ssDNA = single-stranded DNA.
† $P < 0.05$ versus vehicle-treated mice, by chi-square test.

rebamipide-treated mice. In addition, we confirmed the dose-dependent decrease in phosphorylation of IκB in CD4+ T cells from mice treated with rebamipide as compared with vehicle-treated controls (Figure 2D). Furthermore, nuclear translocation of NF-κB subunits (RelA and p65) in CD4+ T cells from rebamipide-treated mice had decreased remarkably compared with that in cells from vehicle-treated controls (Figure 2D).

**Inhibitory effects of rebamipide on T cell activation.** We next examined whether the therapeutic effect of oral administration of rebamipide on thymectomized NFS/*sld* mice was attributable to the inhibition of T cell activation. Cervical lymph node cells and spleen cells were purified from thymectomized NFS/*sld* mice treated with rebamipide or vehicle from ages 4 weeks to 8 weeks. In rebamipide-treated mice, the number of CD4+ and CD8+ T cells from the lymph node and spleen did not change with oral administration of rebamipide at either dose (Figure 3A).

We next examined CD25, CD44, CD62L, and CD69 expression on CD4+ T cells because these makers are known to be highly expressed on activated T cells and memory T cells (28). We found a decreased expression of CD4+,CD62L$^{low}$ effector T cells in lymph nodes from mice treated with rebamipide, as compared with those from the control group (Figure 3A). In contrast, the expression of these markers on splenic CD4+ T cells from rebamipide-treated mice was similar to that in splenic CD4+ T cells from vehicle-treated controls (Figure 3A). It has recently been demonstrated that autoimmunity could be induced by specific in vivo expansion of CD4+,CD62L$^{low}$ effector T cells (29).

**Inhibitory effects of rebamipide on T cell proliferation and cytokine production.** We previously reported that CD4+ T cells from thymectomized mice responded to the α-fodrin peptide JS-1 (25). Thus, we examined whether the rebamipide treatment affects the JS-1–specific proliferative response of splenic CD4+ T cells. A significant decrease in autoantigen (JS-1)–specific T cell proliferation was observed in CD4+ T cells treated with rebamipide (Figure 3B, top left). These results suggest that rebamipide treatment reduced the expansion of JS-1–specific T cells in mice, which is consistent with the low levels of CD4+,CD62L$^{low}$ effector T cells in the rebamipide-treated mice. The proliferative response of anti-CD3 and anti-CD28 mAb-stimulated CD4+ T cells was also decreased by the addition of rebamipide in a dose-dependent manner (Figure 3B, top right). Furthermore, when CFSE-labeled CD4+ T cells were stimulated with anti-CD3 and anti-CD28 mAb in the presence of rebamipide for 72 hours, cell division was suppressed by rebamipide (Figure 3B, bottom).

To confirm the inhibitory effect of rebamipide, an in vitro cytokine assay was performed using splenic CD4+ T cells stimulated with anti-CD3 and anti-CD28. We obtained clear evidence that rebamipide treatment inhibited the production of Th1 (IL-2 and IFNγ), but not Th2 (IL-4 and IL-10), cytokines (Figure 3C). In serum samples, we detected no IL-2, IL-4, or IFNγ in mice treated with rebamipide (data not shown).

It was still unclear whether the antigen-specific T cell response in a normal mouse strain is inhibited by rebamipide. Therefore, CFSE-labeled T cells from OT-2 mice transgenic for ovalbumin-specific T cell receptor

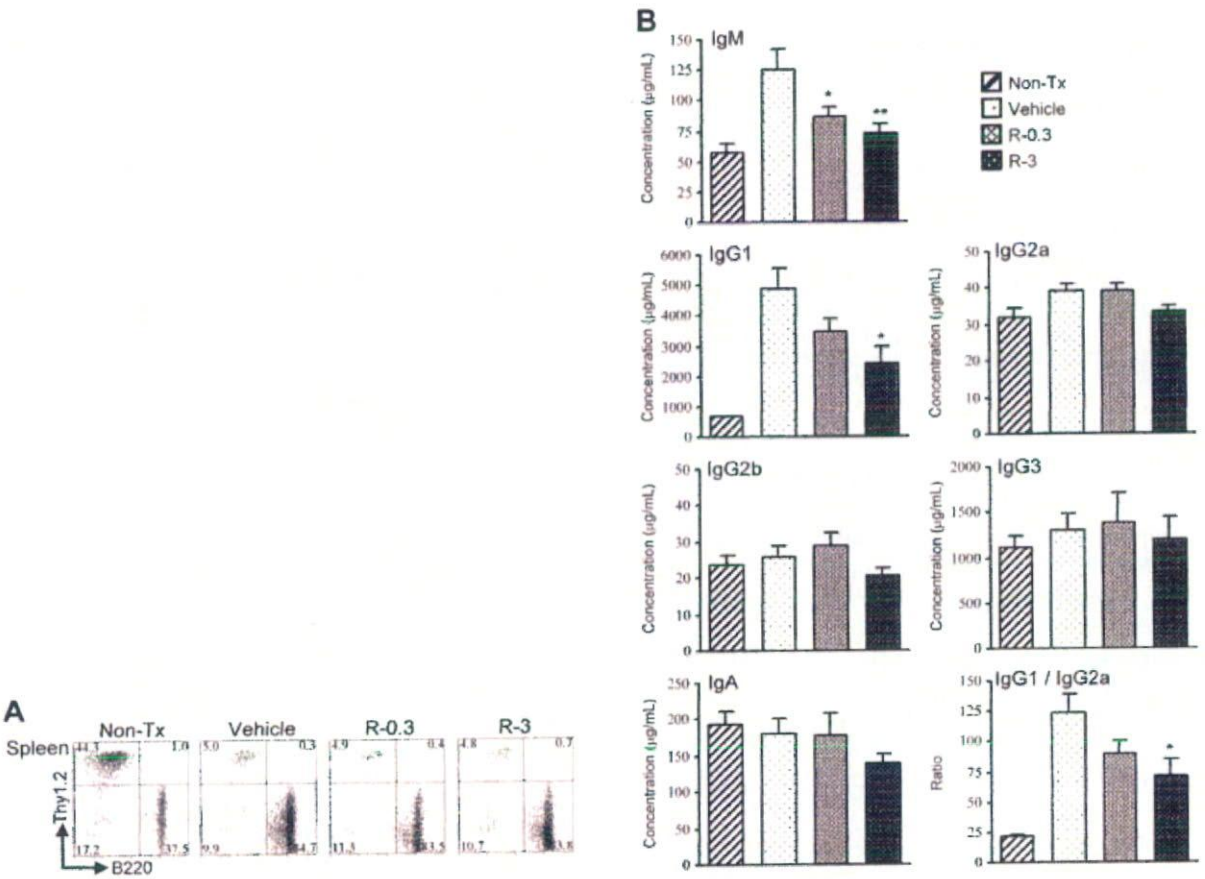


**Figure 4.** Effect of rebamipide on B cell function in the NFS/*sld* mouse model of Sjögren's syndrome after treatment with rebamipide. Mice underwent thymectomy on day 3 after birth and were treated with vehicle, 0.3 mg/kg of rebamipide (R-0.3), or 3 mg/kg of rebamipide (R-3) from age 4 weeks to age 8 weeks. A group of nonthymectomized (non-Tx), vehicle-treated mice was also studied. **A,** Thy1.2+ and B220+ cell subsets in the spleen of the 4 groups of mice, as determined by flow cytometry. Numbers shown in each compartment are the percentage of positive cells. Results are representative of 10–12 mice per group. **B,** Serum concentrations of immunoglobulin subclasses in the 4 groups of mice, as determined by enzyme-linked immunosorbent assay. Values are the mean and SEM of 10 mice per group. * = $P < 0.05$; ** = $P < 0.01$ versus the vehicle-treated group, by Dunnett's test.

were transferred into B6 (Ly5.1+) mice, and ovalbumin peptide was injected into the mice together with rebamipide. Treatment with rebamipide resulted in a dose-dependent inhibition of ovalbumin-specific T cell expansion in vivo (Figure 3D).

**Reduced serum autoantibody production with rebamipide treatment.** Sera were collected after rebamipide and vehicle treatment to evaluate the production of autoantibodies. Thymectomized NFS/*sld* mice have high titers of serum autoantibody against recombinant α-fodrin protein (JS-1) (25). We examined whether oral administration of rebamipide affected serum levels of autoantibody against α-fodrin in this mouse model of SS. As shown in Table 1, the titer of autoantibody against α-fodrin (JS-1) was considerably lower in mice treated with rebamipide than in mice treated with vehicle. The decreased serum titer of autoantibody against α-fodrin suggests that oral administration of rebamipide affected the autoimmune pathology and was able to suppress the systemic production of α-fodrin–specific autoantibody. We also examined serum titers of autoantibodies that are often associated with SS: anti-SSA/Ro, anti-SSB/La, anti-ssDNA, and anti–α-fodrin (30–33). Serum titers of anti-SSA/Ro and anti-SSB/La autoantibodies were significantly decreased in mice treated with rebamipide, but titers of anti–α-fodrin were not statistically significantly different from those in the control mice (Table 1).

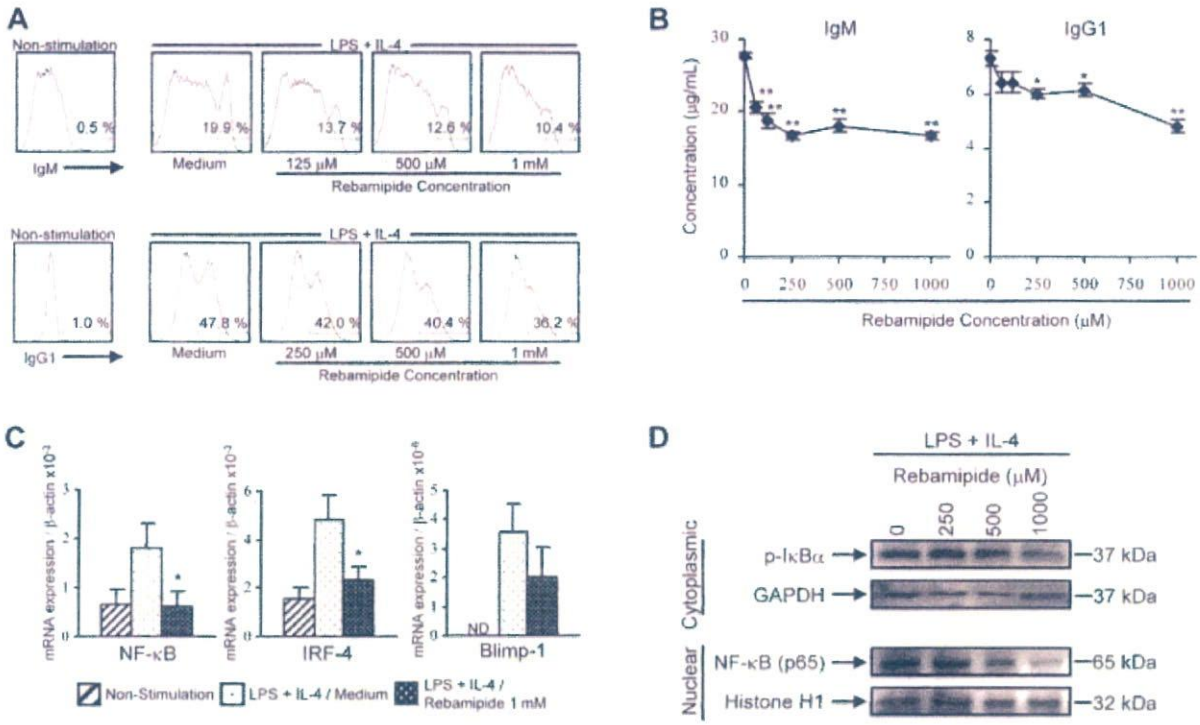


**Figure 5.** Effect of rebamipide on immunoglobulin production in the NFS/*sld* mouse model of Sjögren's syndrome. Mice underwent thymectomy on day 3 after birth and were treated with 3 mg/kg of rebamipide from age 4 weeks to age 8 weeks. **A,** Cell surface expression of IgM and IgG1, as detected by flow cytometry. Enriched splenic B cells were left unstimulated or were stimulated with lipopolysaccharide (LPS) and interleukin-4 (IL-4) in the presence of the indicated concentrations of rebamipide for 5 days. Values are the percentage of positive cells. **B,** Secretion of IgM and IgG1 into supernatants from B cells stimulated for 5 days with LPS and IL-4 in the presence of the indicated concentrations of rebamipide, as detected by enzyme-linked immunosorbent assay. Values are the mean ± SEM of 10 mice. * = $P < 0.05$; ** = $P < 0.01$ versus medium alone, by Dunnett's test. **C,** Expression of mRNA for NF-κB, interferon regulatory factor 4 (IRF-4), and B lymphocyte–induced maturation protein 1 (BLIMP-1), by stimulated B cells, as determined by quantitative reverse transcription–polymerase chain reaction analysis. Results are representative of 3 independent experiments. Values are the mean and SEM expression relative to β-actin mRNA in triplicate wells. * = $P < 0.05$ versus medium alone, by Student's *t*-test. ND = not detected. **D,** Phosphorylation of IκB and nuclear translocation of NF-κB in cytoplasmic and nuclear extracts of activated B cells treated with LPS and IL-4 in the presence of rebamipide, as analyzed by Western blotting. GAPDH and histone H1 were use as the respective internal controls. Results are representative of 3 independent experiments.

**Reduced serum immunoglobulin levels with rebamipide treatment.** In rebamipide-treated mice, the number of splenic B220+ B cells did not change with oral administration of either dose of rebamipide (Figure 4A). We found that thymectomized NFS/*sld* mice developed hypergammaglobulinemia involving both IgG1 and IgM as compared with nonthymectomized control mice (Figure 4B). Rebamipide-treated mice showed prominent inhibition of serum IgM and IgG1 levels ($P < 0.01$), but not the other IgG subclasses or IgA (Figure 4B). This may indicate that oral administration of rebamipide affected all B cell function, which was able to suppress systemic secretion of IgM and IgG1.

**Inhibitory effects of rebamipide on immunoglobulin secretion.** To confirm the inhibitory effects of rebamipide on IgM and IgG1 secretion, we examined the effects of in vitro treatment with rebamipide using splenic B220+ B cells stimulated with LPS and IL-4. We found that rebamipide inhibited B cell production of IgM and IgG1, as determined by flow cytometry (Figure 5A). Rebamipide also inhibited IgM and IgG1 in culture supernatants, as determined by ELISA (Figure 5B). Both of these effects were dose-dependent. Since rebamipide treatment in this mouse model of SS inhibited the production of autoantibodies and immunoglobulins, we also examined the transcriptional activity of NF-κB,

IRF-4, and BLIMP-1. Significant inhibitory effects of rebamipide on the expression of mRNA for NF-κB and IRF-4, transcription factors that are associated with B cell activation and differentiation, were observed (Figure 5C). We confirmed the dose-dependent decrease in phospho-IκB and NF-κB subunits (p65) in activated B cells stimulated with LPS and IL-4 as compared with vehicle-treated controls (Figure 5D).

## DISCUSSION

Since studies of animal models of autoimmune disorders should eventually give rise to appropriate potential treatments in humans with those diseases, it is important to identify the best therapeutic approach by which cells of the immune system can be specifically affected without causing side effects. In this regard, antigen-specific down-regulation of autoimmune processes is considered to be the most suitable therapy (34–36). The findings of the present study of rebamipide treatment in the NFS/*sld* mouse model of Sjögren's syndrome confirm the protective effect of rebamipide on the functional recovery of T cells and B cells in this autoimmune exocrinopathy, probably based on its capacity to inhibit T cell activation and B cell proliferation, in addition to reinforcing the epithelial barrier. Although therapy in SS patients has generally consisted of systemic administration of immunosuppressive or antimuscarinic drugs, it has been known that the systemic use of these drugs induces severe side effects (34). In contrast, it has been reported that oral administration of rebamipide had no clinically significant physical side effects, with normal blood pressure and pulse rate, in healthy adult subjects (37). This study is the first to demonstrate that oral administration of rebamipide effectively inhibits autoimmune pathology in the NFS/*sld* mouse model of SS without causing systemic histopathologic changes.

We previously reported that a cleavage product of 120-kd α-fodrin may be an important autoantigen in the development of primary SS and that anti–120-kd α-fodrin antibodies have been frequently detected in sera from SS patients (25). We have also reported a significant increase in TUNEL+ apoptotic epithelial duct cells in the salivary glands of thymectomized NFS/*sld* mice and a large proportion of FasL in tissue-infiltrating CD4+ T cells (11); both findings support the idea that tissue-infiltrating CD4+ T cells are responsible for tissue destruction, as determined by in vitro cytotoxicity assay. Our data have suggested that one mechanism by which activated CD4+ T cells induce cytotoxicity to salivary gland cells in this murine model of SS is Fas-based and that the primary mediators of the disease are autoantigen-driven T cell responses. In the present study, we found that expression of FasL on CD4+ T cells was significantly inhibited and that TUNEL+ epithelial cell apoptosis declined in the rebamipide-treated mice. A significant decrease in autoantigen-specific T cell proliferation was observed in CD4+ T cells with rebamipide treatment. This is consistent with the finding that rebamipide treatment resulted in the dose-dependent inhibition of ovalbumin-specific T cell expansion in vivo.

In addition, we observed that rebamipide treatment induced a selective impairment of CD4+,CD62L$^{low}$ effector T cells in the lymph nodes. This population was more potent than the population of CD4+,CD62L$^{high}$ cells in inducing a self-directed immune response, as demonstrated by cytometric isolation and adoptive transfer experiments. The induction of autoimmunity by specific in vivo expansion of CD4+,CD62L$^{low}$ cells has recently been demonstrated (29), indicating that CD4+,CD62L$^{low}$ effector T cells may be attractive targets for immune interventions in the treatment of autoimmune diseases. On the other hand, rebamipide treatment did not influence the frequency of CD4+,CD25+ natural regulatory T cells in cervical lymph nodes (data not shown). It is noteworthy that rebamipide treatment inhibited T cell proliferation and Th1 cytokine production (IL-2 and IFNγ). These data indicate that rebamipide treatment effectively inhibits autoimmune pathology in the NFS/*sld* mouse model of SS.

The improvement in secretory function after treatment with rebamipide, as demonstrated by saliva volumes, strongly points to the ingestive mechanism of action of rebamipide. With regard to the small discrepancy between the histologic features of the lacrimal glands and the lacrimal gland function, as demonstrated by tear flow volumes after treatment of rebamipide (see Figure 1), it has been reported that inflammatory lesions in the lacrimal gland develop later than those in the salivary gland in our mouse model (22). It is also possible that the effects of rebamipide on salivary gland cells may be different from the effects on lacrimal gland cells.

The beneficial effects of rebamipide on the epithelial barrier, which have previously been demonstrated in the gastric and small intestinal mucosa (38,39), have possibly, although not definitively, also been shown for the salivary gland epithelia, although the findings are not definitive. While the mechanism of action of rebamipide

on epithelial permeability, which has mostly been studied in the stomach, is not completely understood, it could be related to the capacity of rebamipide to act as a scavenger of cytokine-induced hydroxyl radicals (40) or to induce prostaglandin production (41). Since we found decreased apoptosis of salivary gland epithelia in rebamipide-treated mice, it is possible that the protective effect of rebamipide on the salivary gland epithelia could also account for its beneficial effect on ulcerative colitis in humans or on Dextran sulfate sodium–induced colitis in rats (42). This improvement in the epithelial barrier, together with the capacity of rebamipide to modulate immune responses, may represent a new therapeutic approach to the clinical management of sicca syndrome in SS patients without producing any side effects.

Rebamipide treatment clearly inhibited the production of serum autoantibodies, IgM, and IgG1 and induced a reduction in the transcriptional activity of IRF-4 via down-regulation of NF-$\kappa$B. It has been reported that IRF-4 functions redundantly with IRF-8 to regulate B cell differentiation into immature IgM+ B cells (43). IRF-4 has been shown to regulate the induction of BLIMP-1 expression and BLIMP-1–dependent plasma cell differentiation (44). The majority of IgM and IgG1 are autoreactive and are also reactive with DNA, phosphorylcholine, phosphatidylcholine, and $\alpha$1–3-dextran. The process of autoantibody production in SS is characterized by findings of both an antigen-driven response and a polyclonal B cell activation. The causes of this abnormal activation have not been fully elucidated and are likely to vary in different patients and in different animal models of autoimmune diseases. These diseases are characterized by a high titer of autoantibodies that may play a role in the tissue damage. It is possible that the down-regulatory effect of rebamipide on the immune response would be a good therapeutic approach.

We have previously reported that treatment with anti-CD4 and anti-CD86 mAb, cathepsin S inhibitor, caspase inhibitor, and cyclosporin A improved the autoimmune pathology in this mouse model of SS (11,45–48). In the present study, we observed less drastic effects of rebamipide on histologic features, as compared with those in previous therapeutic experiments. This may be related to the relatively low degree of inhibitory effects on T cell–mediated immune responses. Although we did not simply compare the efficacy of rebamipide with that of systemic administration of a different agent, this successful therapeutic effect of rebamipide would provide the possibility of establishing a new form of therapy for patients with autoimmune symptoms caused by SS as well as other types of diseases.

## ACKNOWLEDGMENTS

The authors thank Ai Nagaoka, Hiroyo Amo, and Satoko Yoshida for technical assistance.

## AUTHOR CONTRIBUTIONS

Dr. Hayashi had full access to all of the data in the study and takes responsibility for the integrity of the data and the accuracy of the data analysis.

**Study design.** Kohashi, Ishimaru, Hayashi.
**Acquisition of data.** Kohashi, Arakaki.
**Analysis and interpretation of data.** Kohashi.
**Manuscript preparation.** Kohashi, Ishimaru, Hayashi.
**Statistical analysis.** Kohashi.

## REFERENCES

1. Fox RI. Sjögren's syndrome. Lancet 2005;366:321–31.
2. Fox RI, Stern M, Michelson P. Update in Sjögren syndrome. Curr Opin Rheumatol 2000;12:391–8.
3. Kruize AA, Smeenk RJ, Kater L. Diagnostic criteria and immunopathogenesis of Sjögren's syndrome: implications for therapy. Immunol Today 1995;16:557–9.
4. Sebzda E, Mariathasan S, Ohteki T, Jones R, Bachmann MF, Ohashi PS. Selection of the T cell repertoire. Annu Rev Immunol 1999;17:829–74.
5. Starr TK, Jameson SC, Hogquist KA. Positive and negative selection of T cells. Annu Rev Immunol 2003;21:139–76.
6. Wakeland EK, Liu K, Graham RR, Behrens TW. Delineating the genetic basis of systemic lupus erythematosus. Immunity 2001;15:397–408.
7. Yasutomo K. Pathological lymphocyte activation by defective clearance of self-ligands in systemic lupus erythematosus. Rheumatology (Oxford) 2003;42:214–22.
8. Marrack P, Kappler J, Kotzin BL. Autoimmune disease: why and where it occurs. Nat Med 2001;7:899–905.
9. Davidson A, Diamond B. Autoimmune diseases. N Engl J Med 2001;345:340–50.
10. Yasutomo K, Horiuchi T, Kagami S, Tsukamoto H, Hashimura C, Urushihara M, et al. Mutation of DNASE1 in people with systemic lupus erythematosus. Nat Genet 2001;28:313–4.
11. Saegusa K, Ishimaru N, Yanagi K, Mishima K, Arakaki R, Suda T, et al. Prevention and induction of autoimmune exocrinopathy is dependent on pathogenic autoantigen cleavage in murine Sjögren's syndrome. J Immunol 2002;169:1050–7.
12. Bieganowska KD, Ausubel LJ, Modabber Y, Slovik E, Messersmith W, Hafler DA. Direct ex vivo analysis of activated, Fas-sensitive autoreactive T cells in human autoimmune disease. J Exp Med 1997;185:1585–94.
13. Miranda-Carus ME, Askanase AD, Clancy RM, Di Donato F, Chou TM, Libera MR, et al. Anti-SSA/Ro and anti-SSB/La autoantibodies bind the surface of apoptotic fetal cardiocytes and promote secretion of TNF-$\alpha$ by macrophages. J Immunol 2000;165:5345–51.
14. Avrameas S. Natural autoantibodies: from 'horror autotoxicus' to 'gnothi seauton'. Immunol Today 1991;12:154–9.
15. Toubi E, Etzioni A. Intravenous immunoglobulin in immunodeficiency states: state of the art. Clin Rev Allergy Immunol 2005;29:167–72.
16. Barabas AZ, Cole CD, Barabas AD, Lafreniere R. Production of

a new model of slowly progressive Heymann nephritis. Int J Exp Pathol 2003;84:245–58.
17. Ravetch JV. Fc Receptors. In: Paul WE, editor. Fundamental immunology. 5th ed. Philadelphia: Lippincott Williams & Wilkins; 2003. p. 685–700.
18. McCarthy J, O'Mahony L, O'Callaghan L, Sheil B, Vaughan EE, Fitzsimons N, et al. Double blind, placebo controlled trial of two probiotic strains in interleukin 10 knockout mice and mechanistic link with cytokine balance. Gut 2003;52:975–80.
19. Kishimoto S, Haruma K, Tari A, Sakurai K, Nakano M, Nakagawa Y. Rebamipide, an antiulcer drug, prevents DSS-induced colitis formation in rats. Dig Dis Sci 2000;45:1608–16.
20. Bamba H, Ota S, Kato A, Miyatani H, Kawamoto C, Yoshida Y, et al. Effect of rebamipide on prostaglandin receptors-mediated increase of inflammatory cytokine production by macrophages. Aliment Pharmacol Ther 2003;18 Suppl 1:113–8.
21. Hayashi Y, Kojima A, Hata M, Hirokawa K. A new mutation involving the sublingual gland in NFS/N mice: partially arrested mucous cell differentiation. Am J Pathol 1988;132:187–91.
22. Haneji N, Hamano H, Yanagi K, Hayashi Y. A new animal model for primary Sjögren's syndrome in NFS/sld mutant mice. J Immunol 1994;153:2769–77.
23. Ishimaru N, Saegusa K, Yanagi K, Haneji N, Saito I, Hayashi Y. Estrogen deficiency accelerates autoimmune exocrinopathy in murine Sjögren's syndrome through Fas-mediated apoptosis. Am J Pathol 1999;155:173–81.
24. Saito I, Haruta K, Shimuta M, Inoue H, Sakurai H, Yamada K, et al. Fas ligand-mediated exocrinopathy resembling Sjögren's syndrome in mice transgenic for IL-10. J Immunol 1999;162:2488–94.
25. Haneji N, Nakamura T, Takio K, Yanagi K, Higashiyama H, Saito I, et al. Identification of α-fodrin as a candidate autoantigen in primary Sjögren's syndrome. Science 1997;276:604–7.
26. Angelin-Duclos C, Johnson K, Liao J, Lin KI, Calame K. An interfering form of Blimp-1 increases IgM secreting plasma cells and blocks maturation of peripheral B cells. Eur J Immunol 2002;32:3765–75.
27. Dong L, Ito S, Ishii KJ, Klinman DM. Suppressive oligodeoxynucleotides delay the onset of glomerulonephritis and prolong survival in lupus-prone NZB × NZW mice. Arthritis Rheum 2005; 52:651–8.
28. Anderson BE, McNiff J, Yan J, Doyle H, Mamula M, Shlomchik MJ, et al. Memory $CD4^+$ T cells do not induce graft-versus-host disease. J Clin Invest 2003;112:101–8.
29. Amend B, Doster H, Lange C, Dubois E, Kalbacher H, Melms A, et al. Induction of autoimmunity by expansion of autoreactive $CD4^+CD62L^{low}$ cells in vivo. J Immunol 2006;177:4384–90.
30. Franceschini F, Cavazzana I. Anti-Ro/SSA and La/SSB antibodies. Autoimmunity 2005;38:55–63.
31. Hayashi Y, Arakaki R, Ishimaru N. Apoptosis and estrogen deficiency in primary Sjögren syndrome [published erratum appears in Curr Opin Rheumatol 2004;16:753]. Curr Opin Rheumatol 2004;16:522–6.
32. Turkcapar N, Olmez U, Tutkak H, Duman M. The importance of α-fodrin antibodies in the diagnosis of Sjögren's syndrome. Rheumatol Int 2006;26:354–9.
33. Chan EK, Hamel JC, Buyon JP, Tan EM. Molecular definition and sequence motifs of the 52-kD component of human SS-A/Ro autoantigen. J Clin Invest 1991;87:68–76.
34. Nepom GT. Therapy of autoimmune diseases: clinical trials and new biologics. Curr Opin Immunol 2002;14:812–5.
35. Peakman M, Dayan CM. Antigen-specific immunotherapy for autoimmune disease: fighting fire with fire? Immunology 2001; 104:361–6.
36. Fox RI, Maruyama T. Pathogenesis and treatment of Sjögren's syndrome. Curr Opin Rheumatol 1997;9:393–9.
37. Hasegawa S, Sekino H, Matsuoka O, Saito K, Sekino H, Morikawa A, et al. Bioequivalence of rebamipide granules and tablets in healthy adult male volunteers. Clin Drug Investig 2003;23:771–9.
38. Matysiak-Budnik T, de Mascarel A, Abely M, Mayo K, Heyman M, Megraud F. Positive effect of rebamipide on gastric permeability in mice after eradication of Helicobacter felis. Scand J Gastroenterol 2000;35:470–5.
39. Matysiak-Budnik T, van Niel G, Megraud F, Mayo K, Bevilacqua C, Gaboriau-Routhiau V, et al. Gastric Helicobacter infection inhibits development of oral tolerance to food antigens in mice. Infect Immun 2003;71:5219–24.
40. Naito Y, Yoshikawa T, Tanigawa T, Sakurai K, Yamasaki K, Uchida M, et al. Hydroxyl radical scavenging by rebamipide and related compounds: electron paramagnetic resonance study. Free Radic Biol Med 1995;18:117–23.
41. Yamasaki K, Kanbe T, Chijiwa T, Ishiyama H, Morita S. Gastric mucosal protection by OPC-12759, a novel antiulcer compound, in the rat. Eur J Pharmacol 1987;142:23–9.
42. Makiyama K, Takeshima F, Kawasaki H, Zea-Iriarte WL. Anti-inflammatory effect of rebamipide enema on proctitis type ulcerative colitis: a novel therapeutic alternative. Am J Gastroenterol 2000;95:1838–9.
43. Lu R, Medina KL, Lancki DW, Singh H. IRF-4,8 orchestrate the pre-B-to-B transition in lymphocyte development. Genes Dev 2003;17:1703–8.
44. Klein U, Casola S, Cattoretti G, Shen Q, Lia M, Mo T, et al. Transcription factor IRF4 controls plasma cell differentiation and class-switch recombination. Nat Immunol 2006;7:773–82.
45. Saegusa K, Ishimaru N, Yanagi K, Haneji N, Nishino M, Azuma M, et al. Treatment with anti-CD86 costimulatory molecule prevents the autoimmune lesions in murine Sjögren's syndrome (SS) through up-regulated Th2 response. Clin Exp Immunol 2000;119: 354–60.
46. Hayashi Y, Ishimaru N, Arakaki R, Tsukumo S, Fukui H, Kishihara K, et al. Effective treatment of a mouse model of Sjögren's syndrome with eyedrop administration of anti-CD4 monoclonal antibody. Arthritis Rheum 2004;50:2903–10.
47. Tsubota K, Saito I, Ishimaru N, Hayashi Y. Use of topical cyclosporin A in a primary Sjögren's syndrome mouse model. Invest Ophthalmol Vis Sci 1998;39:1551–9.
48. Saegusa K, Ishimaru N, Yanagi K, Arakaki R, Ogawa K, Saito I, et al. Cathepsin S inhibitor prevents autoantigen presentation and autoimmunity. J Clin Invest 2002;110:361–9.

# Visualizing the dynamics of p21$^{Waf1/Cip1}$ cyclin-dependent kinase inhibitor expression in living animals

Naoko Ohtani*†, Yuko Imamura*, Kimi Yamakoshi*, Fumiko Hirota‡, Rika Nakayama§, Yoshiaki Kubo¶, Naozumi Ishimaru¶, Akiko Takahashi*, Atsushi Hirao||**, Takatsune Shimizu††, David J. Mann‡‡, Hideyuki Saya††, Yoshio Hayashi¶, Seiji Arase¶, Mitsuru Matsumoto‡, Kazuki Nakao§, and Eiji Hara*†

*Institute for Genome Research, ‡Institute for Enzyme Research, and ¶Institute of Health Biosciences, University of Tokushima, Tokushima 770-8503, Japan; §Center for Developmental Biology, RIKEN, Kobe 650-0047, Japan; ||Cancer Research Institute, Kanazawa University, Kanazawa 920-0934, Japan; **CREST, Japan Science and Technology Agency, Tokyo 102-0075, Japan; ††Institute for Advanced Medical Research, Keio University School of Medicine, Tokyo 160-8582, Japan; and ‡‡Division of Cell and Molecular Biology, Imperial College London, London SW7 2AZ, United Kingdom

Communicated by Thaddeus P. Dryja, Harvard Medical School, Boston, MA, July 25, 2007 (received for review May 11, 2007)

**Although the role of *p21$^{Waf1/Cip1}$* gene expression is well documented in various cell culture studies, its *in vivo* roles are poorly understood. To gain further insight into the role of *p21$^{Waf1/Cip1}$* gene expression *in vivo*, we attempted to visualize the dynamics of *p21$^{Waf1/Cip1}$* gene expression in living animals. In this study, we established a transgenic mice line (p21-*p*-luc) expressing the firefly luciferase under the control of the *p21$^{Waf1/Cip1}$* gene promoter. In conjunction with a noninvasive bioluminescent imaging technique, p21-*p*-luc mice enabled us to monitor the endogenous *p21$^{Waf1/Cip1}$* gene expression *in vivo*. By monitoring and quantifying the *p21$^{Waf1/Cip1}$* gene expression repeatedly in the same mouse throughout its entire lifespan, we were able to unveil the dynamics of *p21$^{Waf1/Cip1}$* gene expression in the aging process. We also applied this system to chemically induced skin carcinogenesis and found that the levels of *p21$^{Waf1/Cip1}$* gene expression rise dramatically in benign skin papillomas, suggesting that *p21$^{Waf1/Cip1}$* plays a preventative role(s) in skin tumor formation. Surprisingly, moreover, we found that the level of *p21$^{Waf1/Cip1}$* expression strikingly increased in the hair bulb and oscillated with a 3-week period correlating with hair follicle cycle progression. Notably, this was accompanied by the expression of p63 but not p53. This approach, together with the analysis of *p21$^{Waf1/Cip1}$* knockout mice, has uncovered a novel role for the *p21$^{Waf1/Cip1}$* gene in hair development. These data illustrate the unique utility of bioluminescence imaging in advancing our understanding of the timing and, hence, likely roles of specific gene expression in higher eukaryotes.**

aging | cell cycle | hair cycle | imaging

The founding member of the mammalian cyclin-dependent kinase (CDK) inhibitor family, p21$^{Waf1/Cip1}$, is one of the best characterized transcriptional targets of the p53 tumor suppressor protein (1–4). As a general inhibitor of CDKs, p21$^{Waf1/Cip1}$ prevents phosphorylation of the retinoblastoma tumor suppressor protein (pRb) thereby enhancing its growth suppressive function (2, 3, 5). Thus, p21$^{Waf1/Cip1}$ links the p53 pathway to the pRb pathway, providing a tight security network toward tumor suppression. Indeed, the tumor-suppressive role of p21$^{Waf1/Cip1}$ is well documented in various cell culture studies; up-regulation of the *p21$^{Waf1/Cip1}$* gene expression participates in processes such as DNA damage-induced cell cycle arrest, cellular senescence, and terminal differentiation, each of which may prevent tumor formation (5, 6). However, *in vivo*, the role of p21$^{Waf1/Cip1}$, especially in the context of tumor suppression, remains unclear. For example, mutations in the *p21$^{Waf1/Cip1}$* gene are rarely observed in human cancers (7), and, although the majority of mice lacking the *p53* gene develop spontaneous tumors by 6 months of age (8, 9), mice lacking the *p21$^{Waf1/Cip1}$* gene do not exhibit any predisposition to spontaneous tumor formation (10, 11). These observations raise a question of whether the results seen in cell culture truly reflect the physiological roles of p21$^{Waf1/Cip1}$ *in vivo*. However, because knockout experiments performed to date have used mice with germ-line deficiencies at the *p21$^{Waf1/Cip1}$* gene locus, there is the possibility of developmental compensation, as seen with other cell cycle regulators (12, 13). Moreover, expression of the *p21$^{Waf1/Cip1}$* gene overlaps with that of other CDK inhibitor family members in many different tissues (5). It is, therefore, possible that the effects of *p21$^{Waf1/Cip1}$* deficiency is somewhat compromised by developmental or somatic compensation by functionally related CDK inhibitors in *p21$^{Waf1/Cip1}$* knockout mice. Alternative approaches are therefore needed to supplement the *in vitro* studies and assist in understanding the physiological roles of *p21$^{Waf1/Cip1}$* gene expression *in vivo*.

Bioluminescence imaging (BLI) is an emerging approach that is based on detection of light emission from cells or tissues (14, 15). Optical imaging by bioluminescence allows a noninvasive and real-time analysis of various biological responses, such as gene expression, proteolytic processing, or protein–protein interactions, in living animals (16–20). In this study, we generated a transgenic mice line (p21-*p*-luc) expressing the firefly luciferase under the control of the *p21$^{Waf1/Cip1}$* gene promoter. Using this mouse model, we explored the dynamics of *p21$^{Waf1/Cip1}$* gene expression in many different biological processes *in vivo*. This approach, in conjunction with the analysis of *p21$^{Waf1/Cip1}$* knockout mice, uncovered a previously uncharacterized function of *p21$^{Waf1/Cip1}$* gene expression in hair development. The ability to image *p21$^{Waf1/Cip1}$* gene expression noninvasively therefore provides a valuable tool for studies on the role of *p21$^{Waf1/Cip1}$* gene expression *in vivo*.

## Results

To study how *p21$^{Waf1/Cip1}$* gene expression is regulated *in vivo*, we attempted to visualize the transcriptional activity of the *p21$^{Waf1/Cip1}$* gene in living animals. To this end, a transgenic mice line (p21-*p*-luc mice) expressing the firefly luciferase

Author contributions: N.O. and Y.I. contributed equally to this work; N.O. and E.H. designed research; N.O., Y.I., K.Y., F.H., R.N., Y.K., N.I., A.T., A.H., and T.S. performed research; N.O., D.J.M., H.S., Y.H., S.A., M.M., K.N., and E.H. analyzed data; and N.O. and E.H. wrote the paper.

The authors declare no conflict of interest.

Freely available online through the PNAS open access option.

Abbreviations: CDK, cyclin-dependent kinase; pRb, retinoblastoma tumor suppressor protein; BLI, bioluminescence imaging.

†To whom correspondence may be addressed. E-mail: ohtani@genome.tokushima-u.ac.jp or hara@genome.tokushima-u.ac.jp.

This article contains supporting information online at www.pnas.org/cgi/content/full/0706949104/DC1.





www.pnas.org/cgi/doi/10.1073/pnas.0706949104

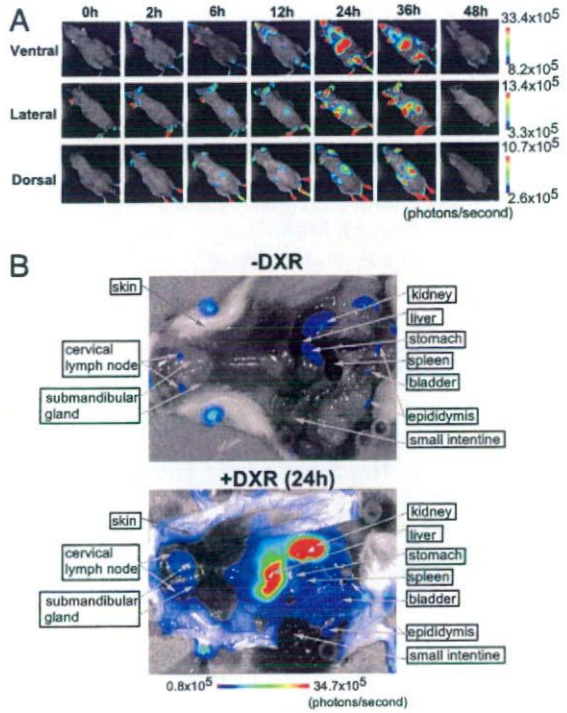


Fig. 1. Characterization of the p21-*p*-luc mice. (*A*) The p21-*p*-luc mice (8-week-old) were injected i.p. with doxorubicin (DXR) (20 mg/kg) and were subjected to noninvasive BLI at various times after doxorubicin (DXR) injection. Representative images of five different experiments are shown. (*B*) The same line of p21-*p*-luc mice were treated with doxorubicin (+DXR) (20 mg/kg) or saline (−DXR) for 24 h, injected with luciferin, and incised through the mouth and anus under anesthesia. Representative BLI data of five different experiments are shown. The color bar indicates photons with minimum and maximum threshold values.

driven by the $p21^{Waf1/Cip1}$ gene promoter, which contains two p53-binding sites, was established and subjected to noninvasive *in vivo* BLI. Although basal levels of bioluminescent signals were very low throughout the body, except for the paws, a striking increase in signal was observed (particularly over the abdomen) within 24 h of treatment with doxorubicin, a DNA damaging agent that activates p53 (Fig. 1*A*). These signals were sustained until 36 h and then declined to baseline values within the next 12 h (Fig. 1*A*, 48 h). To define the organs expressing high levels of luciferase activity, the same lines of transgenic mice were treated with or without doxorubicin for 24 h, injected with luciferin, and incised through mouth and anus under anesthesia (Fig. 1*B*). As expected from noninvasive BLI data (Fig. 1*A*, 24 h), a significant induction of bioluminescent signal was observed in liver and kidney in doxorubicin-treated mice [Fig. 1*B* and supporting information (SI) Fig. 4*A*]. A substantial but less pronounced induction was observed in the submandibular gland, spleen, bladder, and stomach (Fig. 1*B* and SI Fig. 4*A*). Similar but different dynamics of $p21^{Waf1/Cip1}$ gene expression was observed by x-ray irradiation (SI Fig. 5). Importantly, the levels of bioluminescent signal were well correlated with those of endogenous $p21^{Waf1/Cip1}$ mRNA (SI Figs. 4 and 5), indicating that, in the p21-*p*-luc mice, luciferase expression accurately reports the transcriptional dynamics of $p21^{Waf1/Cip1}$ gene expression *in vivo*. Furthermore, in concordance with the levels of endogenous $p21^{Waf1/Cip1}$ expression, luciferase activity was strikingly increased in the cortex and medulla of the kidney (SI Fig. 6). Taken together, these results suggest that the p21-*p*-luc mice provide an ideal tool for the analysis of $p21^{Waf1/Cip1}$ gene expression *in vivo*.

Although p53 serves the beneficial function of tumor suppression, p53 activation may, in some circumstance, act in a manner detrimental to the long-term homeostasis of living organism (21). Indeed, aberrant activation of p53 is known to accelerate the aging process in mice, and the induction of $p21^{Waf1/Cip1}$ gene expression has been shown to be involved this process (22, 23). We thus next attempted to explore the dynamics of $p21^{Waf1/Cip1}$ gene expression throughout entire life span in p21-*p*-luc mice (SI Fig. 7). Unexpectedly, only a slight (3- to 4-fold) induction of bioluminescent signal was observed in aged kidney but not in other aged organs or tissues (SI Fig. 7). Surprisingly, moreover, any signs of strong activation of p53 and DNA damage responses were not observed in aged kidney (SI Fig. 7), indicating that the induction of $p21^{Waf1/Cip1}$ gene expression in aged kidney is likely to be regulated by a p53-independent mechanism, although we cannot rule out the possibility that weak activation of p53 contributes to the up-regulation of $p21^{Waf1/Cip1}$ gene expression.

The up-regulation of $p21^{Waf1/Cip1}$ gene expression is implicated in cellular senescence, the state of stable cell cycle arrest provoked by diverse stresses including DNA damage and oncogenic *ras* expression in cultured primary cells (4, 24). To explore this notion *in vivo*, p21-*p*-luc mice were subjected to a conventional chemically induced skin tumor protocol with a single dose of DMBA for initiation and biweekly treatment with 12-*o*-tetradecanoylphorbol 13-acetate (TPA) for promotion. Because this protocol causes an oncogenic mutation in the H-*ras* gene, it appeared to be ideal for studying physiological responses against oncogenic *ras* expression in living animals (25, 26). In agreement with previous reports (25, 26), benign skin papillomas began to appear after 7–8 weeks of promotion (Fig. 2*A*). Notably, papilloma formation was accompanied by the induction of a bioluminescence signal (Fig. 2*A*), endogenous $p21^{Waf1/Cip1}$ expression, and activation of p53 (Fig. 2*B*). These observations, together with previous studies that indicate that disruption of the $p21^{Waf1/Cip1}$ gene results in an increase of papilloma formation or carcinoma formation (27–29), strongly suggest that $p21^{Waf1/Cip1}$ plays a preventative role against oncogenic *ras*-signaling *in vivo*.

Because noninvasive BLI permits continuous readout of gene expression in living animals (14, 15), we next examined the kinetics of $p21^{Waf1/Cip1}$ gene expression toward papilloma formation. To our surprise, a remarkable bioluminescent signal was observed well before papilloma appearance and oscillated with a 3-week period (Figs. 2 *C* and *D*). Unexpectedly, moreover, a remarkable expression of endogenous $p21^{Waf1/Cip1}$ was observed in the hair bulb, but not in the skin itself (Fig. 2*E*), suggesting that $p21^{Waf1/Cip1}$ may play a role in hair development. To produce new hairs, existing hair follicles undergo cycles of growth (anagen), regression (catagen), and rest (telogen) (30). Because TPA treatment has been shown to promote entry of hair follicles into their anagen phase (31), we next asked whether the oscillating bioluminescence signal in DMBA/TPA-treated skin reflects hair follicle cycle progression. Although TPA treatment, in itself, did not cause skin papilloma formation, a similar oscillation of bioluminescence signals and $p21^{Waf1/Cip1}$ mRNA expression was induced by TPA treatment alone (SI Fig. 8). Notably, this was accompanied by remarkable hair growth (SI Fig. 8*A*), suggesting a role for $p21^{Waf1/Cip1}$ in the hair follicle cycle progression in mouse skin.

To substantiate this idea in a more physiological setting, we next tested whether $p21^{Waf1/Cip1}$ expression oscillates throughout the natural hair follicle cycle, exploiting the fact that hair follicle cycles are synchronized for the first two postnatal periods of hair follicle growth in mice (32). Although the dynamics of hair cycle progression were visually undetectable during the second postnatal hair follicle cycle, BLI was sensitive enough to monitor oscillating $p21^{Waf1/Cip1}$ expression (Fig. 3*A*). The levels of biolu-

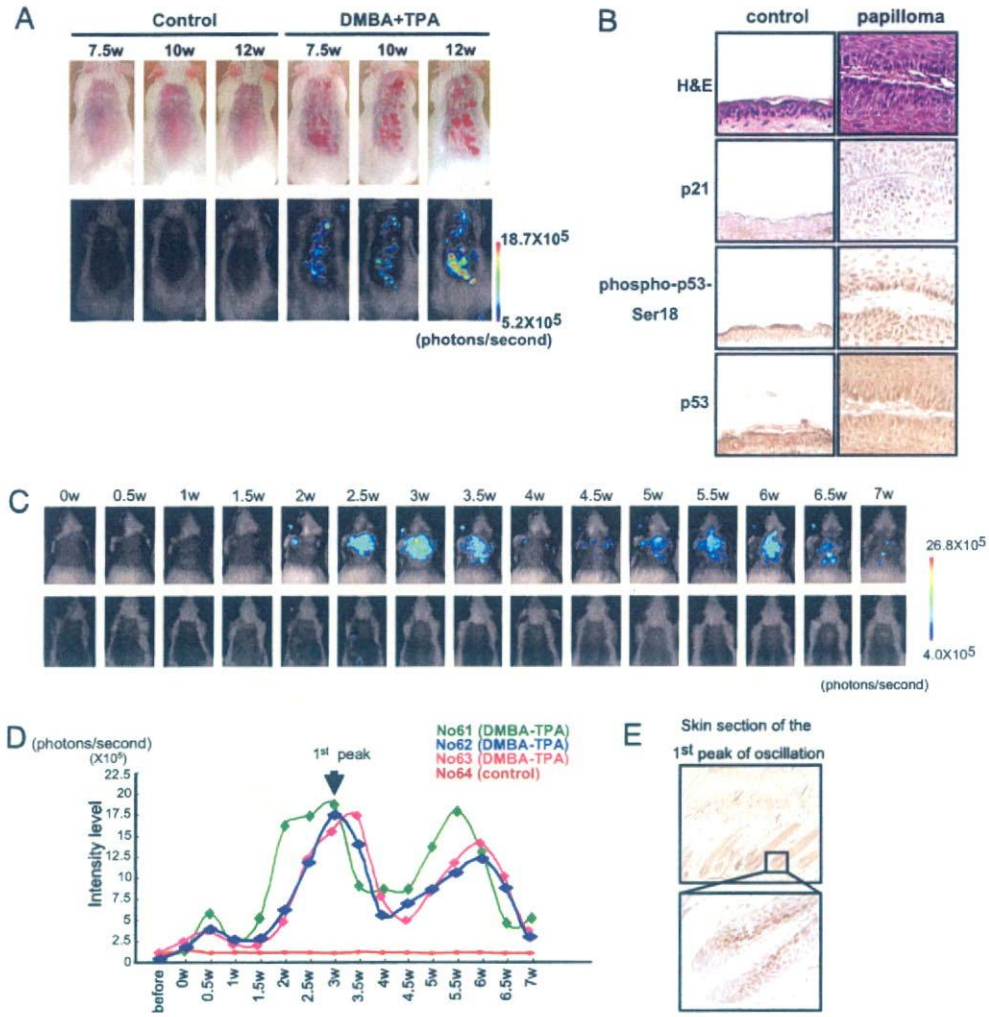


**Fig. 2.** Oscillation of bioluminescence signals in DMBA/TPA-treated mouse skin. (*A*) The p21-*p*-luc mice treated with DMBA/TPA or with acetone (control) were subjected to noninvasive BLI at indicated time points after TPA treatment. Representative images of 12 different experiments were shown (*Lower*). These papillomas and control skin were photographed in regular lighting (*Upper*). The color bar indicates photons with minimum and maximum threshold values. (*B*) H&E staining and the immunohistochemistry for endogenous $p21^{Waf1/Cip1}$ expression, phosphorylation of p53 at serine 18 residue, and p53 expression were performed by using biopsy samples of skin papilloma (*Right*) or control normal skin (*Left*). (*C*) Noninvasive BLI was performed throughout the time course after DMBA/TPA treatment (*Upper*) or acetone control (*Lower*). Mice were imaged at 0.5-week intervals after TPA treatment. Representative images of 12 different experiments were shown. The color bar indicates photons with minimum and maximum threshold values. (*D*) The intensity of bioluminescence signal throughout the time course was graphed. (*E*) Immunohistochemistry was conducted to examine the endogenous $p21^{Waf1/Cip1}$ expression in the dorsal skin at 3 weeks after TPA treatment (corresponding to the first peak of bioluminescence oscillation). A magnified image of hair bulb is shown (*Lower*).

minescence signals reached their peak at postnatal day 28 (P28); endogenous $p21^{Waf1/Cip1}$ expression was also strongly observed in the precortex area above the hair matrix (differentiating cell area) at this time (Fig. 3*A*). These data suggest that $p21^{Waf1/Cip1}$ may regulate the size of hair bulb and thereby control the hair phenotype.

To explore this possibility, microscopic examination of the various hair types was conducted by using mice with different $p21^{Waf1/Cip1}$ genotypes (10). The morphology of the four main hair types (guard, awl, auchene, and zigzag) was not significantly different among three different genotypes ($p21^{+/+}$, $p21^{+/-}$, $p21^{-/-}$) (data not shown). However, the proportion of zigzag hairs, which are produced by the smallest hair bulb, was significantly reduced in $p21^{+/-}$ mice, whereas awl hairs and auchene hairs, which are produced by the intermediate-sized hair bulb, were increased (Fig. 3*B*). Curiously, these effects were less pronounced in $p21^{-/-}$ mice (Fig. 3*B*). Importantly, however, unusually high level of $p27^{Kip1}$ expression, another member of the $p21^{Waf1/Cip1}$ family CDK inhibitors, was observed in the hair bulb of $p21^{-/-}$ mice (Fig. 3*C*). Thus, it is likely that the effects of $p21^{Waf1/Cip1}$ deficiency are concealed, at least in part, by up-regulation of $p27^{Kip1}$ expression in the hair bulb of $p21^{-/-}$ mice. In line with this observation, the proportion of zigzag hairs has been shown to reduce in $p27^{Kip1}$ knockout mice (33), suggesting that $p21^{Waf1/Cip1}$ and $p27^{Kip1}$ possess overlapping role(s) in hair development.

It is worthwhile to note that a similar level of $p21^{Waf1/Cip1}$ expression was observed in anagen hair bulbs, regardless of p53 gene status (SI Fig. 9*A*). Moreover, the proportion of four main hair types was not substantially different among mice of three different genotypes ($p53^{+/+}$, $p53^{+/-}$, $p53^{-/-}$) (SI Fig. 9*B*), suggesting that p53 is not a major player in this setting. Interestingly, although we were unable to see any p53 expression in the hair bulb throughout hair follicle cycle (data not shown), the levels of

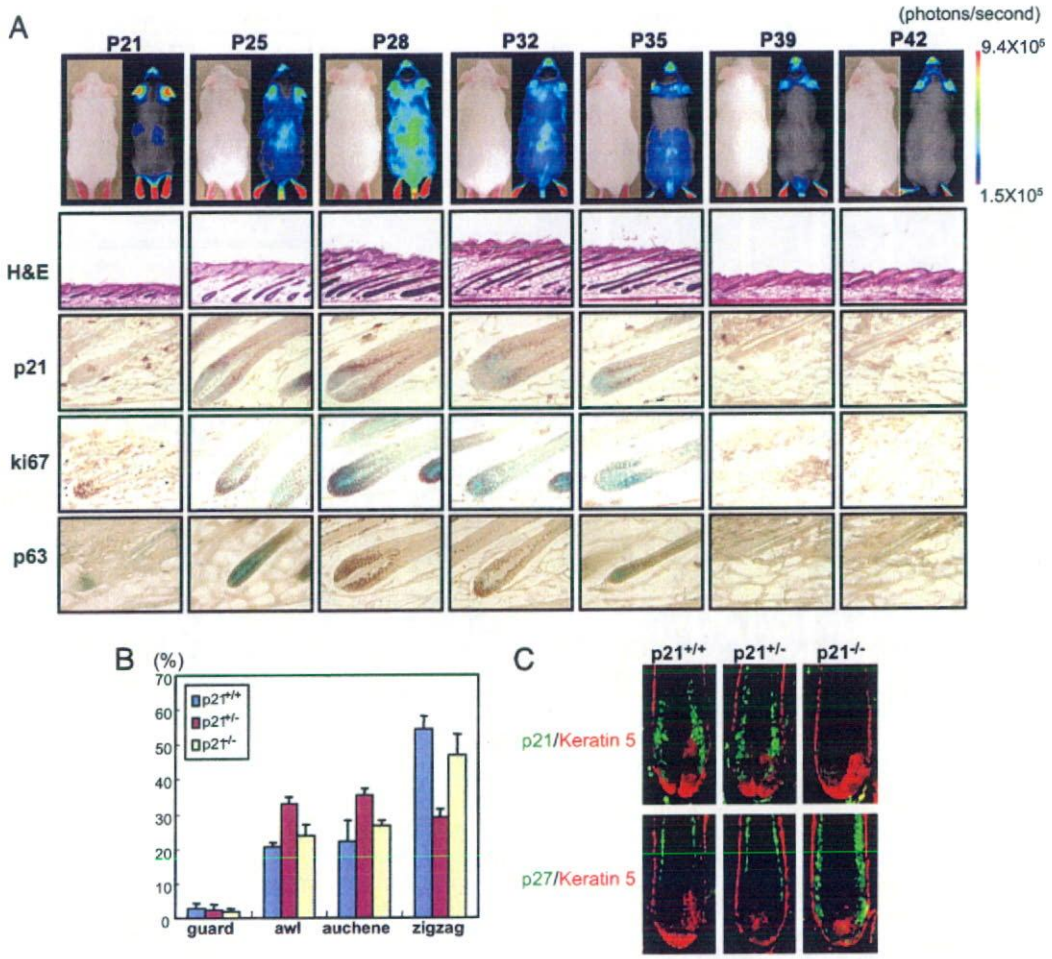


**Fig. 3.** Real-time imaging of hair follicle cycle oscillation in living mice. (*A*) The p21-*p*-luc mice were subjected to noninvasive BLI from postnatal day 21 (P21) to P42. Representative images of five different experiments are shown at the top. The color bar indicates photons with minimum and maximum threshold values. At the indicated time point of postnatal development, dorsal skin of p21-*p*-luc mice was harvested and processed for H&E staining or for immunohistochemistry. (*B*) Summary of the prevalence of hair phenotypes in mice of different $p21^{Waf1/Cip1}$ genotype (C57BL/6 background). The means ± SD of three independent experiments are shown. (*C*) Immunofluorescence of dorsal skin section from P28 mice was performed by using antibodies against $p21^{Waf1/Cip1}$ (green) or $p27^{Kip1}$ (green). Keratin 5 (red) was used as a marker for outer root sheath.

p63 (34), a member of p53-family of transcription factors, were dramatically increased in anagen hair bulbs (Fig. 3*A*). Together, these results imply that p63, but not p53, may play a critical role in the regulation of hair development.

## Discussion

In this study, we generated a transgenic mouse model to visualize $p21^{Waf1/Cip1}$ gene expression in living animals. The p21-*p*-luc mice carry the firefly luciferase cDNA under the control of the $p21^{Waf1/Cip1}$ gene promoter. Because this promoter contains two canonical p53-binding sites, this mouse model is expected to be an ideal system for monitoring not only $p21^{Waf1/Cip1}$ gene expression, but also p53 activation *in vivo*. Indeed, a dramatic induction of bioluminescent signal was observed in various organs within 24 h upon treatment with doxorubicin, a well known DNA-damaging agent that activates p53 (Fig. 1 and SI Fig. 4). Notably, different dynamics of $p21^{Waf1/Cip1}$ gene expression were observed when p21-*p*-luc mice were irradiated with x-ray (SI Fig. 5). In both cases, the levels of bioluminescent signals observed were well correlated with those of endogenous $p21^{Waf1/Cip1}$ mRNA detected by RT-PCR analysis (Fig. 1 and SI Figs. 4 and 5), indicating that the p21-*p*-luc mice provide an ideal tool to monitor the expression of $p21^{Waf1/Cip1}$ gene and/or activity of p53 in living animals. Interestingly, neither doxorubicin nor x-rays induced $p21^{Waf1/Cip1}$ gene expression in the small intestine, implying that p53 is not a major regulator of $p21^{Waf1/Cip1}$ gene expression in the small intestine, as suggested by previous studies (35).

By monitoring and quantifying $p21^{Waf1/Cip1}$ gene expression repeatedly in the same mouse throughout its entire life span, we revealed the dynamics of $p21^{Waf1/Cip1}$ gene expression during the aging process in living mice. Only a slight (3- to 4-fold) induction of bioluminescent signal was observed in kidney, but not in other organs, as mice age (SI Fig. 7). Moreover, strong signs of p53 activation and DNA damage responses were virtually undetectable in aged kidney (SI Fig. 7). These results were unexpected because several lines of evidence suggest that p53-dependent induction of $p21^{Cip1/Waf1}$ is involved in the aging process (22, 23, 36). Our results are, however, consistent with a recent RT-PCR-based study showing that only a slight increase in the $p21^{Waf1/Cip1}$ gene expression was seen in tissues from old mice versus young mice (37, 38). Moreover, it has been shown that increased p53 expression under the endogenous p53 gene promoter protects mice from tumorigenesis without showing any indication of